ARTICLES

Sol−Gel Preparation of AuCu and Au_4Cu Nanocluster Alloys in Silica Thin Films

Ji-Hye Gwak, Sung-Jin Kim, and Minyung Lee*

Department of Chemistry, Ewha Womans University, Seoul 120-750, Korea

Received: January 26, 1998; In Final Form: June 17, 1998

Using sol−gel processing and high-temperature annealing, metal alloy nanoclusters of AuCu and Au_4Cu in SiO_2 thin films were synthesized. The crystallographic data show that the lattice parameters of those nanocluster alloys, both showing the fcc structure, are very close to the bulk values. The nanocrystals obtained by annealing at 900 °C were nearly spherical in shape, having the AuCu size of ca. 23 nm in radius and the Au_4Cu size of ca. 35 nm. The peaks of the optical spectra of the samples annealed at 700−900 °C are located at 555 nm for AuCu and at 562 nm for Au_4Cu.

Introduction

Noble metal nanoparticles have been subjected to intensive studies because they have large third-order optical nonlinearities and ultrafast time response in the surface plasmon resonance (SPR) absorption region. For the past few years there are many reports concerning measurements of the third-order nonlinear optical coefficient,[1−9] $\chi^{(3)}$, and dynamics of photoexcited electrons.[10−12] Prerequisite to those studies, linear optical properties of metal particles, influenced by interband transition and surface plasmon resonance, have also drawn considerable attention.[13] The absorption spectra of metal particles arising from the interband transition are altered from those of bulk, owing to the quantum size effect.[14] The SPR absorption of metal nanoclusters is also of interest because its bandwidth and peak position are affected by the nanocrystal size. The peak position of the surface plasmon resonance is predicted by the well-known Mie resonance condition

$$\epsilon'_m(\omega_s) + 2\epsilon_d(\omega_s) = 0 \quad (1)$$

where ϵ'_m is the real part of the dielectric constant of the metal particle, ϵ_d the dielectric constant of the surrounding dielectrics, and ω_s the surface plasmon resonance frequency. According to eq 1, the SPR band depends on both metal species and composition of surrounding dielectrics. Pure noble metal nanoparticles such as silver, gold, and copper show the different SPR bands in the ultraviolet−visible region. The SPR absorption peak of Ag, Au, and Cu in silica matrix occurs approximately at 400, 530, and 570 nm, respectively. It has been experimentally confirmed that changing the matrix to titania, which has a larger dielectric constant than silica, shifts the SPR band of metal nanoparticles to longer wavelength. In case of gold, a 110−170 nm red shift has been observed.[15,16] There was also an attempt to fabricate SiO_2−TiO_2 thin films containing noble metal nanoparticles with which the continuous tuning of absorption is viable in this wavelength range.[17] Motivation for those studies stems partly from the fact that controlling optical absorption of third-order nonlinear optical materials is, in general, very important from the viewpoint of their practical application.

It is natural to think that the alloy form will give different SPR bands because their dielectric constants are expected to be different from those of the pure form. This will provide a new way of tuning the optical absorption of the nanocomposites. Although noble metal nanoparticles in pure form have been widely investigated and a lot of useful information including linear and nonlinear optical properties has been accumulated, the studies on alloy nanoclusters are relatively rare. Among noble metal alloys, Ag and Au are completely miscible in bulk. The SPR peak of Ag_xAu_{1-x} changes monotonically from pure Au(510 nm) to pure Ag(405 nm) for increasing x.[18] Compared to Ag and Au, silver and copper are less miscible in bulk. Ag and Cu nanocluster alloys were reported by Magruder et al., who used the high-energy ion-implantation method.[19] On the other hand, it has been observed that Ag and Cu particles prepared by the sol−gel method exist as independent particles without forming "alloys".[20] Concerning gold and copper, there is one report by Baglioni and co-workers who synthesized $AuCu_3$ nanocluster alloy having 1−10 nm diameters, using the reverse micelle method.[21] The work was only focused on preparation of gold and copper alloy nanoparticles, and no attention was paid to the optical property of the alloy.

This work concerns the preparation, microstructure, and optical properties of gold and copper nanocluster alloys in silica matrices. It has been known that in bulk Au and Cu form various alloys with different compositions such as AuCu, $AuCu_3$, $AuCu_4$, Au_3Cu, Au_4Cu, etc.[22] It is important to understand the microstructure of those alloys and, moreover, to unravel the surface plasmon absorption region by carefully choosing the composition of Au and Cu. In this context, we first synthesized AuCu and Au_4Cu alloy nanoclusters in SiO_2 matrices, using sol−gel processing and high-temperature heat treatment. The crystal structure was studied by X-ray crystallography, and the crystal size was measured by high-resolution TEM. Surface plasmon absorption of those metal alloy clusters as a function

* To whom correspondence should be addressed. Tel: 82-2-360-2383. Fax: 82-2-360-2384. E-mail: mylee@mm.ewha.ac.kr.

S1089-5647(98)00887-6 CCC: $15.00
Published on Web 09/15/1998

of heat-treatment temperature was characterized by optical spectroscopy.

Experimental Procedure

For the synthesis, tetraethyl orthosilicate (TEOS, 98%) was bought from ACROS. $HAuCl_4 \cdot 4H_2O$ and $Cu(NO_3)_2 \cdot 3H_2O$ were bought from Showa Chemical Inc. The solution containing TEOS, distilled water, 1-propanol, and 2-butanol was first prepared with molar ratio of 1:8.12:6.7:4.0. $HAuCl_4$ and $Cu(NO_3)_2$ were added to the solution and were vigorously stirred for 10 min. A molar ratio of Au and Cu for AuCu and for Au_4Cu was maintained as 1:1 and 4:1, respectively. The molar ratio of metal (Au plus Cu) with respect to TEOS was 0.196. The aged solution was spin-coated on a silica glass plate (25×25 mm^2). The sample was heat-treated at 250 °C in air for 90 min and subsequently heat-treated in H_2 at 500−900 °C for 5 h at a 100 °C interval. By this method, the prepared thin films, looking brownish or red-brownish, appeared to be homogeneous and defect-free. By omitting the procedure of adding metal salts, a blank sample was also prepared.

The sample's absorption spectra in 300−800 nm region were recorded at each heat-treated temperature, using the blank sample as a reference.

X-ray diffraction data were obtained by the Cu Kα line from an X-ray diffractometer (Siemens D500). The diffraction signal from nanocrystals is weak, so the data were collected for 1 h.

The TEM data were obtained by a Hitachi analytical transmission electron microscope (model H-9000) that has 0.18 nm point resolution and 0.1 nm lateral resolution. The TEM sample was prepared in the following way. Two 4×4 mm plates were prepared by cutting the sample. The quartz plates were glued using epoxy in such a way that the coated sides faced each other. Two dummy silicon wafers having the same size were also prepared, and each was pasted on the outer side of the sample. The coated film was centered on a 3 mm diameter circle and was cut to make a cylinder type. Then a 100 μm thick disk was prepared by cutting the cylinder parallel to the cross section and by thinning as well as polishing. Final thinning to give electron transparency was achieved by ion-milling with a single Ar gun at 5 keV. In this way of sample preparation for TEM, it is possible to measure the film thickness as well as the particle size.

Results

AuCu Alloy Nanoclusters. Figure 1 shows the XRD data of a AuCu sample. The first diffraction peak occurs at $2\theta = 40.28°$. This corresponds to the (111) plane of the fcc lattice structure. The broad background arises from the amorphous silica matrix. A bulk AuCu crystal has three different crystal structures, orthorhombic, tetragonal, and face-centered cubic-(fcc), depending on the preparing condition such as temperature. Our data indicate that the alloy form having the fcc structure is only formed by the sol−gel processing. The calculated lattice constant from the X-ray data is 3.872 ± 0.007 Å. The diffraction intensity increases as the heat-treatment temperature increases. This means that higher processing temperature leads to better crystallinity and larger particle size. For the temperature range of 500−700 °C, the peak shape is not symmetric, owing to small amounts of pure Au metal particles that coexist with AuCu. Gold starts to form nanoclusters at a lower temperature than copper does.[8] The Au nanoparticle also has the fcc lattice structure, but its lattice constant is larger than that of the Au/Cu alloy. Therefore, the diffraction peak by pure gold nanoparticles appears at the smaller angle.

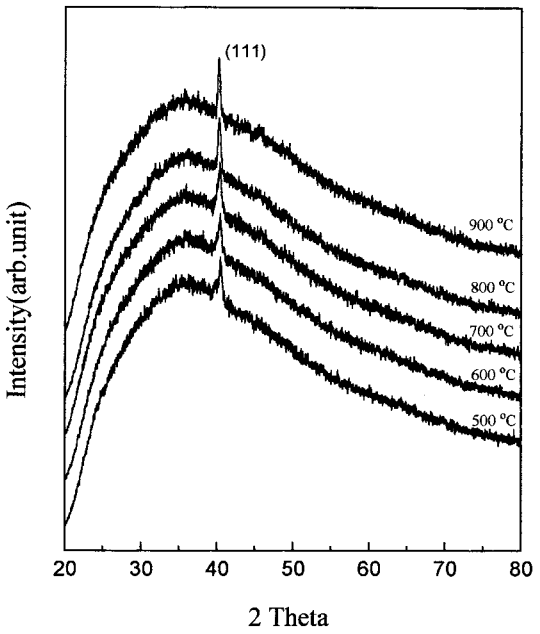

Figure 1. XRD data of the AuCu nanocluster alloy in SiO_2 as a function of heat-treatment temperature.

Figure 2a is the TEM data of the AuCu sample heat-treated at 900 °C. The shape of the sample is spherical, and the average size is ca. 45 nm in diameter. The thickness of the silica thin film is ca. 165 nm. Figure 2b is the electron diffraction pattern of one selected AuCu nanoparticle. The first six diffraction spots consist of a hexagon, indicating the AuCu nanoparticle structure is face-centered cubic. This is consistent with the XRD data shown in Figure 1. The lattice constant value of 3.865 ± 0.009 Å on average was obtained from the electron diffraction pattern.

Figure 3 shows the absorption spectra of AuCu alloy nanoparticles in SiO_2 thin film. Initially the sample was heat-treated at 500 °C and its absorption spectrum was measured. The same procedure was repeated up to 900 °C, by taking the temperature interval of 100 °C. The sample absorption spectra exhibit very different characteristics below and above 700 °C. From 500 to 700 °C, the absorption peak shifts gradually to shorter wavelength. For example, the absorption maximum of the sample heat-treated at 500 °C is located at 594 nm but gradually shifts to 580 nm (600 °C) and 557 nm (700 °C) as the heat-treatment temperature increases. As shown in the X-ray data, the AuCu alloy nanoparticles are already formed at 500 °C.

In the temperature range of 700−900 °C, the absorption spectra show that AuCu nanocrystal formation is complete at 700 °C because the peak position does not change. Further heat treatment above the temperature increases the surface plasmon absorption width and increases the absorbance. The isosbestic point by two absorption spectra recorded at 800 and 900 °C occurs at 460 nm. In the 550−800 nm region where the absorption peak is located, there is about 10% increase in absorbance, when the annealing temperature changed from 800 to 900 °C. Beside the main peak, there is an additional peak around 420 nm that grows as the annealing temperature increases. It may be, albeit unclear at the moment, associated with the interband transition of AuCu metal particles.

Au_4Cu Nanoclusters. Figure 4 shows XRD data of the Au_4Cu sample. Unlike AuCu, three distinct peaks are shown at the diffraction angle $2\theta = 39.03$, 45.43, and 66.16°. Only fcc structure is known for bulk Au_4Cu crystal. Therefore, the peaks

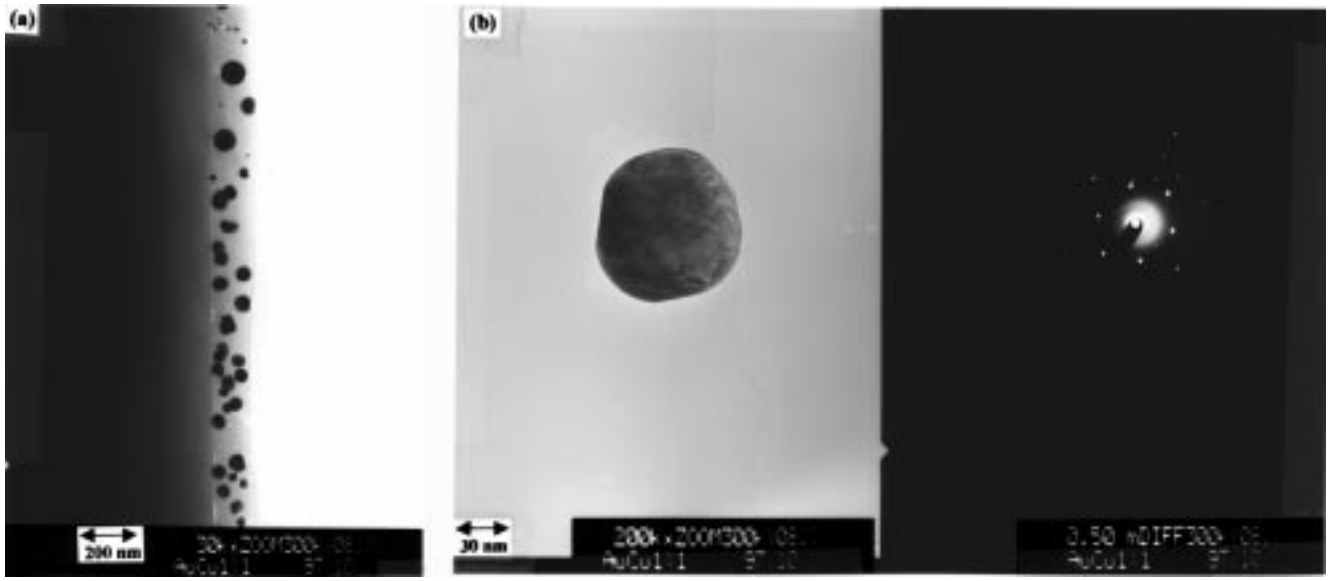

Figure 2. (a) TEM micrograph and (b) electron diffraction pattern of AuCu−SiO_2 samples heat-treated at 900 °C. The camera constant is 9.93 mm Å.

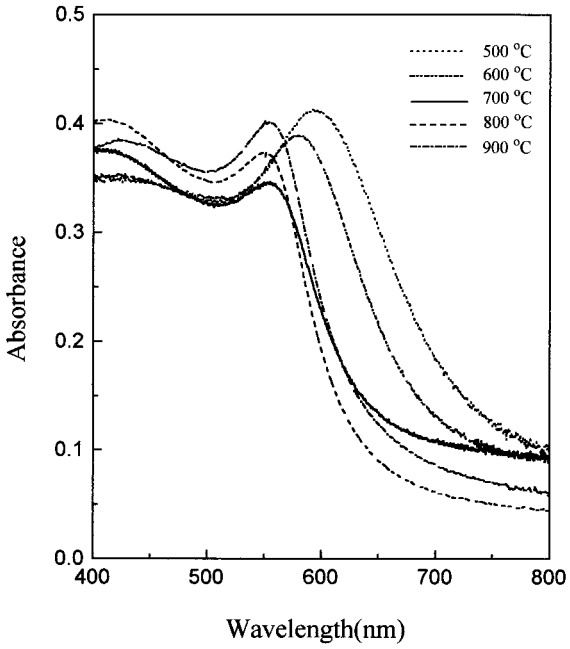

Figure 3. Absorption spectra of the AuCu−SiO_2 sample as a function of heat-treatment temperature.

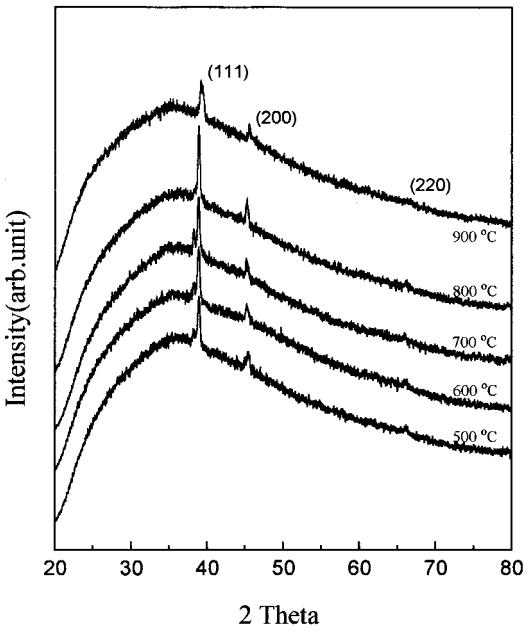

Figure 4. XRD data of the Au_4Cu nanocluster alloy in SiO_2 as a function of heat-treatment temperature.

correspond to the (111), (200), and (220) planes of the fcc structure. The calculated lattice constant from the X-ray data is 3.995 ± 0.002 Å. The diffraction intensity increases as the heat-treatment temperature increases, except for the 900 °C sample. For 500−700 °C data, there is a satellite peak located at $2\theta = 38.27°$. As explained for the AuCu sample, this is due to the presence of pure Au nanometal particles. The satellite peak disappears at 800 °C. Unlike for AuCu, the peak intensity at 900 °C decreases as compared with 800 °C.

Figure 5a is the cross-sectional image data of the TEM micrograph for the Au_4Cu sample heat-treated at 900 °C. The shape of the sample is spherical with the average size of ca. 75 nm in diameter. The thickness of the silica thin film is ca. 165 nm. Figure 5b is the electron diffraction pattern of one selected Au_4Cu nanoparticle. Like the electron diffraction pattern of AuCu, it also shows the hexagonal lattice structure, indicating the Au_4Cu particle has the fcc structure. The TEM analysis on the particle structure is in agreement with the result obtained by XRD. The lattice constant value of 3.991 ± 0.018 Å was obtained from the electron diffraction pattern.

Figure 6 shows the absorption spectra of Au_4Cu alloy nanoparticles in SiO_2 thin film. The temperature dependence of the absorption spectra of Au_4Cu is similar to that of AuCu, but the surface plasmon peak maximum is different. The absorption maximum of the sample heat-treated at 500 °C is located at 619 nm but gradually shifts to 593 nm (600 °C) and 564 nm (700 °C) as the heat-treatment temperature increases. In the temperature range of 700−900 °C, the absorption spectra indicate that Au_4Cu nanocrystal formation is complete at 700 °C because the peak position barely changes. The particle size increases as the heat-treatment temperature increases further because the surface plasmon absorption width increases. The isosbestic point by two absorption spectra recorded at 800 and 900 °C occurs at 540 nm. The peak absorption slightly decreases from 0.36 at 800 °C to 0.34 at 900 °C.

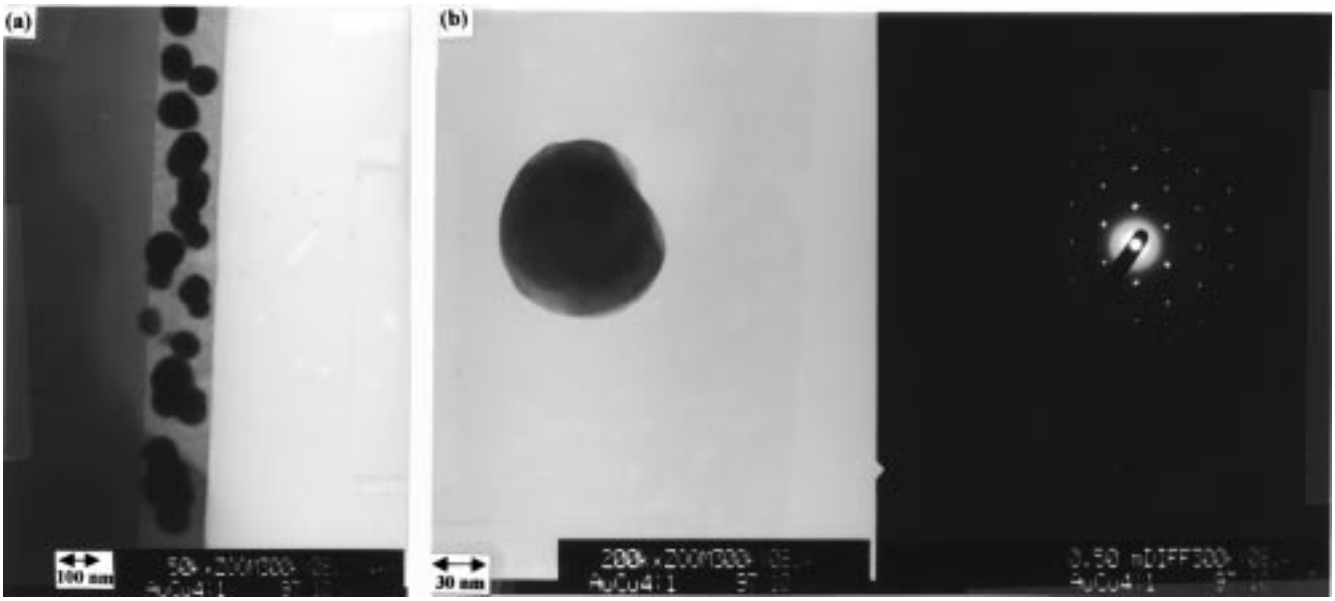

Figure 5. (a) TEM micrograph and (b) electron diffraction pattern of $Au_4Cu-SiO_2$ samples heat-treated at 900 °C. The camera constant is 9.93 mm Å.

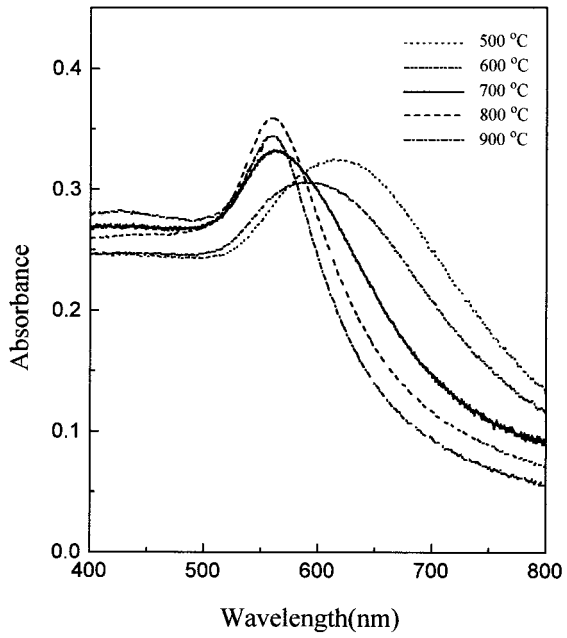

Figure 6. Absorption spectra of the $Au_4Cu-SiO_2$ sample as a function of heat-treatment temperature.

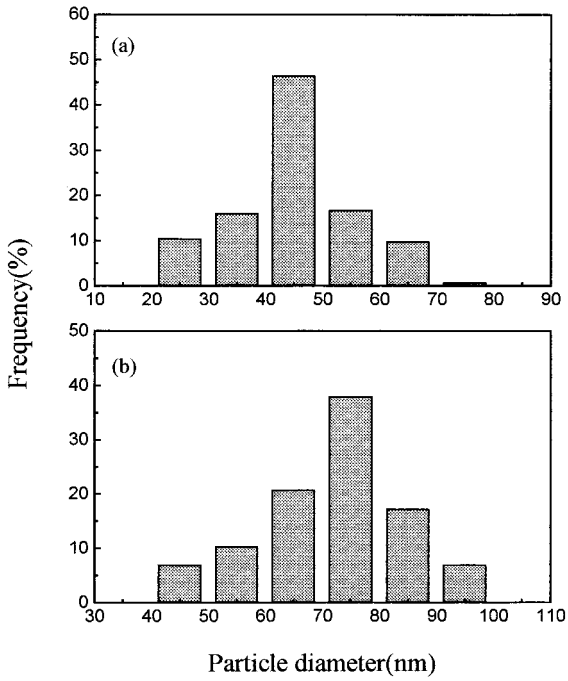

Figure 7. Nanoparticle size distribution taken from TEM data of (a) AuCu and (b) Au_4Cu nanoclusters in SiO_2.

Discussion

The prepared samples of AuCu and Au_4Cu both show the fcc crystal structure. In the temperature range of 500−900 °C, nanocrystal formation of both AuCu and Au_4Cu shows almost the same trend. Under the same preparation conditions, the size of Au_4Cu is larger than that of AuCu. Figure 7 is the size distribution for the samples taken from TEM data. The AuCu covers 20−80 nm centered at 45 nm, while the size distribution of Au_4Cu covers 40−100 nm centered at 75 nm.

XRD is another means to estimate the particle size through Scherrer's equation

$$D = 0.94\lambda/\Delta 2\theta \cos\theta \qquad (2)$$

where D is the particle diameter, λ the X-ray wavelength, and $\Delta 2\theta$ the full width at half-maximum of the peak. X-ray data show that AuCu alloy crystal is well-formed up to 900 °C, but Au_4Cu alloy crystal at 900 °C shows different characteristics such as the peak shift and broadening of the absorption band, compared to those at 800 °C. For this reason, the XRD data of the 800 °C sample were taken for comparison. The calculated nanocluster diameter was 23 nm for AuCu and 31 nm for Au_4Cu. As seen in TEM data, Scherrer's euqation correctly predicts the larger size for Au_4Cu, compared with AuCu. However, the calculated particle sizes by Scherrer's equation are smaller. This difference may be due to the wide distribution of the particle size and the different heat-treatment temperature, because the equation is only exact for the uniform size and the higher heat-treatment temperature is known to give the larger particle size.

The pure gold in silica shows the SPR maximum at 530 nm and the copper at 570 nm. Since the peak positions of absorption spectra of the alloy form of Ag/Au and Ag/Cu are

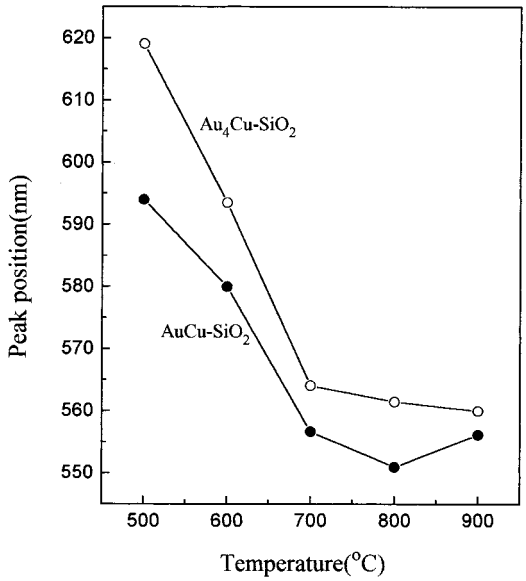

Figure 8. Peak position of absorption spectra of AuCu and Au_4Cu nanoparticles in SiO_2 as a function of heat-treatment temperature.

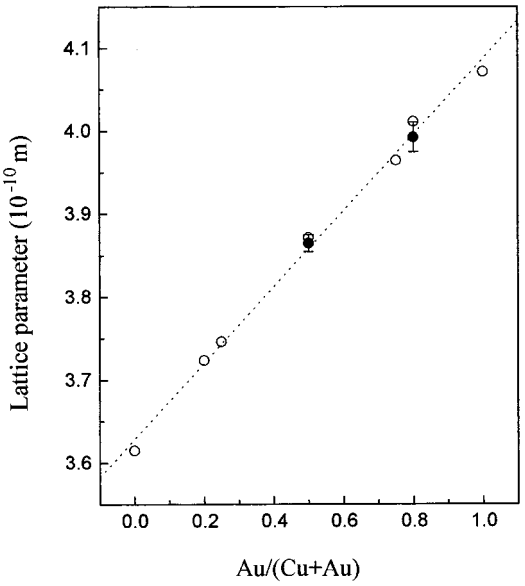

Figure 9. Lattice parameter of AuCu and Au_4Cu nanoclusters in SiO_2 (closed circles). For comparison, those of bulk Au/Cu alloys are also shown as open circles.

located between those of the pure form, the peak position of Au/Cu alloy would be expected to occur between 530 and 570 nm. As shown in Figure 8, the peak position of the SPR band of AuCu and Au_4Cu does not change significantly by the heat-treatment temperature above 700 °C. The similar behavior was observed for pure Cu nanocluster formation.[6] As average values were taken in 700−900 °C, SPR peaks of the alloy nanoparticles are located at 555 ± 3 nm for AuCu and 562 ± 2 nm for Au_4-Cu. A very interesting observation is that the peak position of Au_4Cu is about 7 nm higher than that of AuCu. In case of Ag and Au nanoclusters, the peak position was shifted from 400 to 510 nm as the relative content of Cu increased.[17] A similar behavior was also observed for Ag and Cu nanoclusters that were prepared by the ion-implantation method.[18] It should be mentioned that the optical spectra obtained are not purely due to absorption, but are influenced by scattering, especially for the samples heat-treated at temperatures higher than 700 °C. In other words, the peak position in the absorption spectra originating solely from surface plasmon resonance for AuCu and Au_4Cu alloy nanoclusters could be different from those values obtained in this work.

In making Cu nanoparticles, a cumbersome effect is the presence of the copper oxider layer enclosing the metal surface. The presence of the oxide layer can be identified by a broad absorption around 800 nm. This problem is severe when the copper nanoparticle is made by the reverse micelle method.[23] Under certain conditions, $\epsilon(800)/\epsilon(570)$, in which $\epsilon(\lambda)$ is the extinction coefficient, has been observed up to the value of 0.53. The 570 nm is the peak absorption wavelength of the surface plasmon resonance of Cu. The copper oxide layer does not seem to exist for the AuCu sample annealed at 800−900 °C because the absorption spectra show a plateau near 800 nm. The Au_4Cu sample does not show such a plateau around 800 nm, but this is probably, in part, due to the shift of SPR absorption peak to the red wavelength. For both cases, the absorbance ratio, $\epsilon(800)/\epsilon(\lambda_{max})$, is less than 20%.

The lattice constant of bulk Au is 4.079 Å, and that of Cu is 3.615 Å. The lattice constant of their alloy form lies in the range. As shown in Figure 9, they show a good linear relationship when the lattice parameter was plotted as a function of the molar ratio of Au/(Cu + Au). As shown in the figure, the lattice parameters of alloy nanoclusters are very close to the bulk values. To synthesize alloy particles, Au and Cu ions were mixed exactly as 1:1 for AuCu and 4:1 for Au_4Cu. However, it does not mean that they form alloys following the stoichiometry because the diffusion rate of the ions is different. This has been already noticed in the work on Ag_xAu_{1-x} alloys.[18] A ternary phase diagram of Ag−Au−Cu shows that Au−Cu is less miscible than Ag−Au.[24] This is, in part, due to different atomic radii. The atomic radii of Ag and Au are almost the same (144 pm). The atomic radius of Cu is 128 pm, which is smaller than that of Au. There is also difference in the lattice constant: the lattice constant of pure bulk Au crystal is 4.086 Å, but that of pure Cu is 3.615 Å.[22] Our results prove that, despite these differences, Au and Cu nanocrystal alloys are formed reasonably well, maintaining the good stoichiometric ratio. Because of these novel structural and optical characteristics, compared with pure form or other noble metal alloys, further studies including nonlinear optical properties and electron dynamics of gold and copper alloy nanoclusters may reveal new interesting phenomena.

In summary, metal alloy nanoclusters of AuCu and Au_4Cu in SiO_2 matrices were successfully synthesized using the sol−gel method and high-temperature heat treatment. By TEM it was confirmed that nearly spherical nanoparticles of AuCu having an average diameter of 45 nm and that of Au_4Cu having an average diameter of 70 nm were embedded in SiO_2 thin films. The prepared film thickness was about 165 nm. The crystallographic data show that the lattice parameters of those nanocluster alloys, both showing the fcc structure, are not different from those of the bulk. The peaks of the optical spectra of the samples annealed at 700−900 °C are located at 555 ± 3 nm for AuCu and at 562 ± 2 nm for Au_4Cu, respectively.

Acknowledgment. This work has been financially supported by the academic research fund of Ministry of Education and by KOSEF to S.-J.K. (96-0501-0601-3), Republic of Korea.

Supporting Information Available: Part of the TEM micrographs given in Figures 2 and 5 and the TEM micrograph of the electron diffraction pattern of Au_4Cu (3 pages). Ordering and access information is given on any current masthead page.

References and Notes

(1) Hache, F.; Ricard, D.; Flytzanis, C.; Kreibig, U. *Appl. Phys. A* **1988**, *47*, 347.

(2) Bloemer, M. J.; Haus, J. W.; Ashley, P. R. *J. Opt. Soc. Am. B* **1990**, *7*, 790.

(3) Yang, L.; Becker, K.; Smith, F. M.; Magruder III, R. H. *J. Opt. Soc. Am. B* **1994**, *11*, 457.

(4) Haglund, R. F., Jr.; Yang, L.; Magruder, R. H., III; Wittig, J. E.; Becker, K.; Zuhr, R. A. *Opt. Lett.* **1993**, *18*, 373.

(5) Uchida, K.; Kaneko, S.; Omi, C.; Hata, H.; Asahara, Y.; Ikushima, A. J.; Tokizaki, T.; Nakamura, A. *J. Opt. Soc. Am. B* **1994**, *11*, 1236.

(6) Kundu, D.; Honma, I.; Osawa, T.; Komiyama, H. *J. Am. Ceram. Soc.* **1994**, *77*, 1110.

(7) Puech, K.; Blau, W.; Grund, A.; Bubeck, C.; Cardenas, G. *Opt. Lett.* **1995**, *20*, 1613.

(8) Lee, M.; Kim, T. S.; Choi, Y. S. *J. Non-Cryst. Solids* **1997**, *211*, 143.

(9) Chae, L.; Lee, M.; Kim, H. K.; Moon, D. W. *Bull. Korean Chem. Soc.* **1997**, *18*, 886.

(10) Heilweil, E. J.; Hochstrasser, R. M. *J. Chem. Phys.* **1985**, *82*, 4762.

(11) Roberti, T. W.; Smith, B. A.; Zhang, J. Z. *J. Chem. Phys.* **1995**, *102*, 3860.

(12) Ahmadi, T. S.; Logunov, S. L.; El-Sayed, M. A. *J. Phys. Chem.* **1996**, *100*, 8053.

(13) See, for example: Kreibig, U.; Vollmer, M. *Optical Properties of Metal Clusters*; Springer: Berlin, 1995.

(14) Schaff, T. G.; Schafigullin, M. N.; Khoury, J. T.;Vezmar, I.; Whetten, R. L.; Cullen, W. G.; First, P. N. *J. Phys. Chem. B* **1997**, *101*, 7885.

(15) Kozuka, H.; Zhao, G.; Sakka, S. *J. Sol-Gel Sci. Technol.* **1994**, *2*, 741.

(16) Matsuoka, J.; Yoshida, H.; Nasu, H.; Kamiya, K. *J. Sol-Gel Sci. Technol.* **1997**, *9*, 145.

(17) Innocenzi, P.; Brusatin, G.; Martucci, A.; Urabe, K. *Thin Solid Films* **1996**, *279*, 23.

(18) Sinzig, J.; Radtke, U.; Quinten, M.; Kreibig, U. *Z. Phys. D* **1993**, *26*, 242.

(19) Magruder, R. H., III; Wittig, J. E.; Zuhr, R. A. *J. Non-Cryst. Solids.* **1993**, *163*, 162.

(20) De, G.; Tapfer, L.; Catalano, M.; Battaglin, G.; Caccavale, F.; Mazzoldi, P.; Haglund, R. F. *Appl. Phys. Lett.* **1996**, *68*, 3820.

(21) Sangregorio, C.; Galeotti, M.; Bardi, U.; Baglioni, P. *Langmuir* **1996**, *12*, 5800.

(22) Villars, P.; Calvert, L. D. *Person's Handbook of Crystallographic Data for Intermetallic Phases*; ASM International: Materials Park, OH, 1991.

(23) Lisiecki, L.; Pileni, M. P. *J. Am. Chem. Soc.* **1993**, *115*, 3887.

(24) Villars, P.; Prince, A.; Okamoto, H. *Handbook of Ternary Alloy Phase Diagrams*; ASM International: Materials Park, OH, 1995.